

A 3D RFID Static Test System Using a Spherical Near-Field Antenna Measurement Chamber

Yuan-Hung Lee, Meng-Ying Tsai, Chang-Fa Yang, *Member, IEEE* and Ike Lin

Abstract—This paper presents a method for evaluating radio frequency identification (RFID) 3D readable ranges, implemented by integrating a spherical scanning antenna measurement system for RFID static tests in an anechoic chamber environment. Also presented with demonstrative examples are measurement efficiency in terms of total elapsed measurement time, figures of merit on characterizing the tag readable range of the static test results, and the associated system validations.

Index Terms—RFID, Static Test, Anechoic chamber, Spherical scanning, Readable range

I. INTRODUCTION

RADIO frequency identification (RFID) has been pervasively used in many different applications, such as electric toll collections, bill of material (BOM) managements, and retail commercial products, etc. Thanks to cost reduction of the RFID system and maturity of the internet of things (IoT) technology, the RFID and IoT related industries are growing up and the associated applications are becoming popular [1].

The RF performance of the RFID system is highly sensitive to its operation environments, tag arrangements, reader and tag designs. In this paper, an attempt has been made to build a reliable 3D static test system [2] such that RFID operation performance in three dimensions can be evaluated within a microwave anechoic chamber environment for antenna testing to reduce various interferences from different environments and possibly to obtain parameterized results of RFID performance due to controllable impacting factors in different operation environments. The static test system utilizes a commercial reader as the air interface to access the RFID tags to provide similar measurement environments used in commercial application systems.

In this static testing system development, various testing scenarios based on commercial RFID tags for the validation of the measurement system features had been performed through measuring the associated tag readable range characteristics of the different scenarios. Approaches to improve measurement efficiency based on the results of the different interaction models of the multi-tag characteristics are analyzed and summarized in this paper.

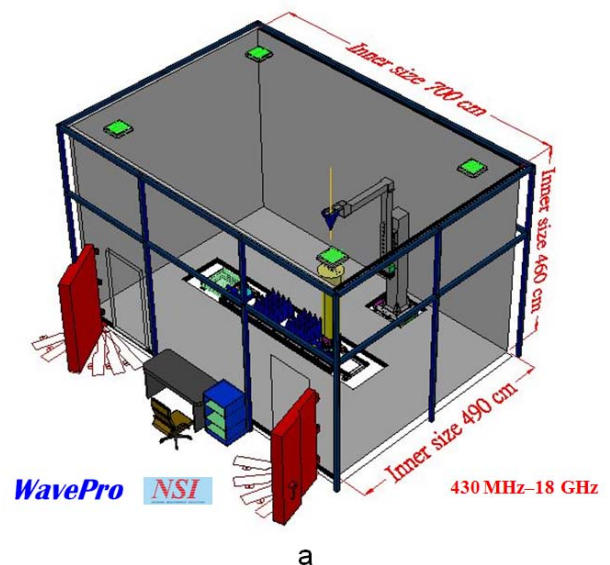
II. SYSTEM CONFIGURATIONS

A. Hardware Environments

In the realistic RFID operation environments, the effect of multipath often causes measurement inaccuracy. In order to mitigate the impact from multipath, this RFID static test system

was built to operate in conjunction with a spherical near-field antenna measurement chamber using an NSI (NearField Systems Inc.) made 3D spherical scanner built in the antenna anechoic testing chamber of National Taiwan University of Science and Technology (Taiwan Tech) for this study, as shown in Fig. 1. The associated operations of the RFID static test system in the anechoic chamber can effectively eliminate multipath effects due to environmental clutters. This system utilizes a dielectric made swing arm to steer the theta angular coordinate of the illuminating direction from the reader/probe antenna pointing to a device under test (DUT) composed of a tag or group of tags. Along with a Styrofoam made DUT supporting mast for steering the associated phi angular coordinate in such a way that performance of the tags along any specific direction over almost the full 3D sphere centered at the origin of the laboratory coordinate system can be made.

Also depicted in Fig. 1(c), a 2D only measurement mode with an extended testing distance up to 3.6 meters in this chamber can be made by rotating the swing arm of the system to the 90 degree theta direction and moving the phi rotating mast horizontally away from the origin so that a back-and-forth motion adjustment of the phi mast can be applied to change the measurement distance between DUT and the reader/probe antenna. A dual polarized wide band probe antenna for frequencies from 430MHz to 18GHz is used to measure the orthogonal field components radiated and responded in between the reader and tags of the RFID system.



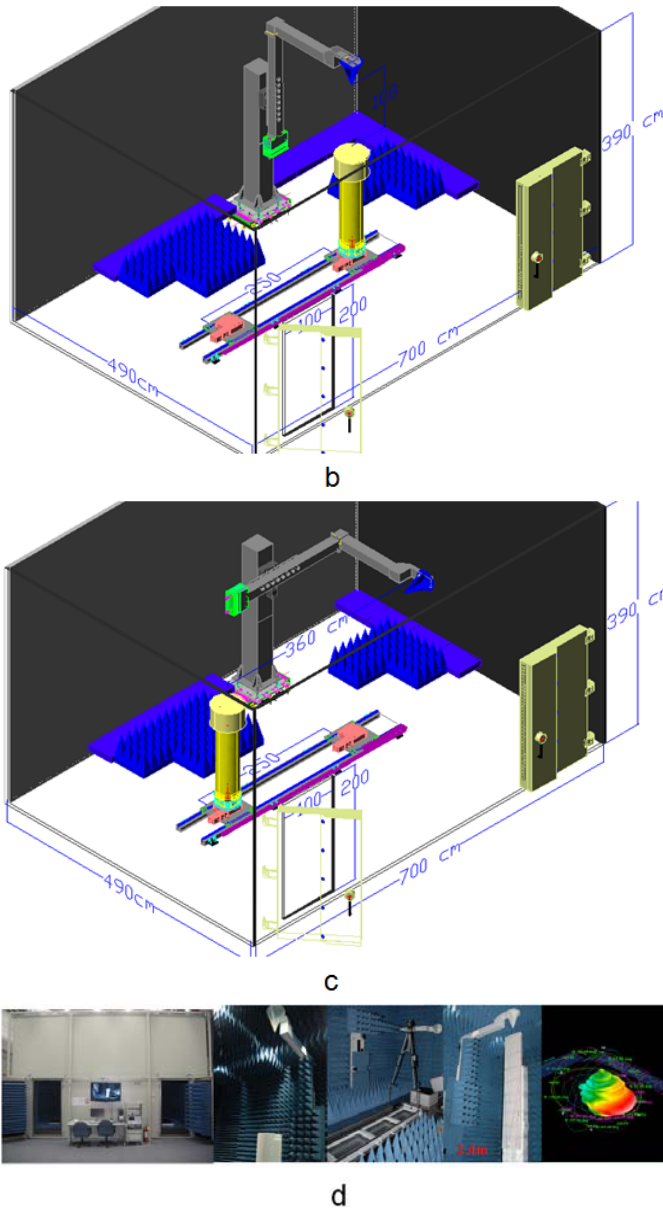


Fig. 1 NSI 3D spherical near-field chamber at Taiwan Tech (a) dimensions (b) 3D mode (c) 2D mode (d) photographs

Besides, as shown in Fig. 2, an Impinj UHF RFID reader is used in this study, although other commercial readers may be employed instead. The Impinj reader is compatible with Low-Level Reader Protocol (LLRP) defined by EPCglobal [3]. Special functions of the Impinj reader can be enhanced through Impinj LLRP extend API [4].

RFID Reader

Impinj Reader V3.2

- LLRP compatible
- Impinj extend LLRP

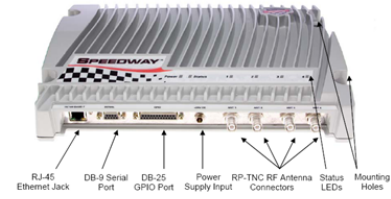


Fig. 2 RFID reader.

B. Architectures

The logical architecture of the static test system is depicted in Fig. 3. The static test system software deployed on a desktop computer controls the theta and phi axes of NSI-700S-90 3D scanner through NSI2000 antenna measurement system software module provided by NSI [5].

The signal attenuation levels between the Impinj reader output port and the probe antenna input ports were measured to be 3.55dB and 3.75dB respectively for the theta and phi polarization paths at 920MHz in this system. A 1dB attenuator is added at the reader output port to reduce the signal output mismatch effect on the reader due to the probe antenna. Also, the probe antenna gains in the theta and phi polarizations are 6.55dBi and 6.15dBi respectively at 920MHz. The gains of the probe antenna and the associated attenuations need to be calibrated in order to determine the tag readable range. Note that the calibration uses data only at 920MHz because the frequency hopping ranges of the UHF RFID system are limited within 5MHz in our system and 26 MHz bandwidth maximum worldwide. Those hopping ranges cause only 0.1dB difference on the calibration for the path loss and the probe antenna gains. Such a small difference is negligible in determining the tag readable range.

If required, the default configuration of the static test system for passive mode antenna performance characterization shown in Fig. 3 can be enabled by redirecting the RF signal path from the probe antenna to the RF I/O port2 of the PNA (performance network analyzer). In this default configuration, a closed RF loop can be made with phase-locked RF signal sent from RF I/O port1 of the PNA, running through the RF cable path of the DUT support mast and then connecting to an impedance matched RF cable fed to the antenna input port of the tag under test. Radiation RF signal transmitted or received by the tag antenna through the dual-polarized probe antenna of this default measurement configuration is then directed to the RF I/O port2 of the PNA network analyzer and makes the whole RF signal path a closed RF loop. The antenna performance of the tag, including realized receiving/transmitting antenna peak gain, gain distribution, and antenna radiation efficiency, can be determined by using the typical 3D antenna measurement methodology in either near-field scanning or far-field scanning approaches as available.

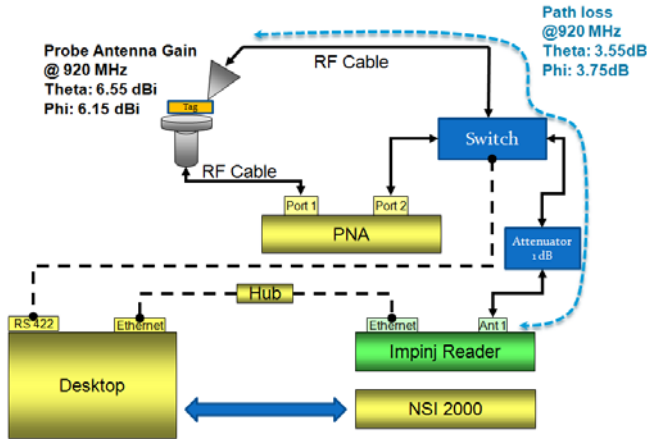


Fig. 3 Logical architecture.

The architecture of the static test system is depicted in Fig. 4. NSI2000 AMS software module is conducted by the static test system through Microsoft InterOP interface to control the motions of the probe antenna and the DUT support mast and also the switch between the theta and phi polarizations of the probe antenna. The static test system uses the LLRP protocol to control the Impinj reader through TCP/IP.

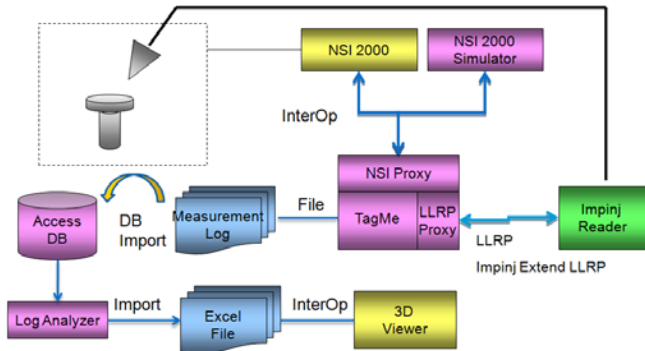


Fig. 4 The architecture of the static test system.

C. Software features

Figure 5 depicts the scope of the measurement methodology in this system. There are two major categories. One is the choice on options of the measurement parameters and the other is the evaluation and characterization of the RFID tag properties.

The measurement parameters are further categorized into four parts, including: 1) field conditions, 2) positioner scan parameters, 3) reader parameters, and 4) middleware parameters, as described below:

- 1) Field Conditions: Two major conditions are considered: the number of tags in the field and the arrangements of tags. The parameter "Number of tags" is required if the testing objective is to acquire the characteristics of the tags related to "detect all" in which all the tags in the field must be identified. The condition on the tag arrangement is required if the testing objective is to acquire the measurement results of the inter-tag interferences under different conditions of

the tag arrangement.

- 2) Positioner Scan Parameters: These include the NSI 3D scanner scan control parameters for measurement angular spans along Theta and Phi directions, angular spacing along Theta and Phi scan directions, and the polarization switching of the probe antenna along vertical (Theta) or horizontal (Phi) field components. The associated scan parameters have been controlled with the NSI 3D scanner software module through which the RFID system performance parameters at specific field component at certain angle of observation within the specified 3D angular coverage can be measured.
- 3) Reader Parameters: The LLRP and the Impinj extend LLRP are applied to control the Impinj reader such that the reader can be activated to build up the communication with tags for all the required tag characteristic evaluations. The system parametric variables to setup LLRP parameters include transmit power, sensitivity, RF mode index, session, tag population, tag transmit time, as depicted in Fig. 5. Unless otherwise specified, all the RFID parameters in this paper use the default values listed in TABLE I.
- 4) Middleware Parameters: Four major factors are parameterized for the evaluation of the measurement accuracy and stability of the static test system which include measurement period, minimum power search algorithm, tag detection criteria and time delay before making measurements.

TABLE I
DEFAULT LLRP PARAMETERS USED IN THIS PAPER

LLRP Parameters	Default Value	Remark
Transmit Power	30dBm	Maximum value by Taiwan regulatory
Sensitivity	0 dB	
RF Mode Index	1000	<ul style="list-style-type: none"> •Divide ratio=8 •EPC TAG T&C conformance=false •M value = FMO •Forward link modulation=PR_ASK •Spectral Mask Indicator=DI •Backscatter data rate in bps=40k •PIE value=1500 •Min tari=6250 •Max tari=6250 •Step tari value=0
Session	0	
Tag Population	Number of Tags in Field	the start Q value to use in Query command
Tag transmit time	0	

For performing measurements, a longer measurement period returns a higher confidence level on measurement results, yet consumes more resources. Three minimum power search algorithms are applied for the optimization of the total measurement period versus measurement accuracy, which include: 1) Each Power Search Algorithm, 2) Hierarchical Search Algorithm, and 3) Binary Search Algorithm. A Tag Detection Criteria is utilized to improve the stability of the measured results by varying the number of the tag read-count. Also, the factor of the time delay before making measurements is used to control the delay period between two successive measurements to prevent possible interferences from the adjacent measurements.

Tag characteristics can be inspected in two categories of the

grouping identity. One category refers to a single tag or each of the tags, and the other refers to a group of the tags. The single tag characteristic is used if only one single tag is to be measured in the field. The each tag characteristic is employed to inspect every individual tag characteristic in the group of the tags and is referred as “Detect Each”. On the other hand, the group of the tags characteristic is required for modeling the multiple tags as a group to study the collective group characteristic instead of every individual tag of the group. In this category, the term “Detect All” is referred in the case that all the tags in the field must be identified, and the term “Detect Any” is referred in the case that any of the tags in the field is identified.

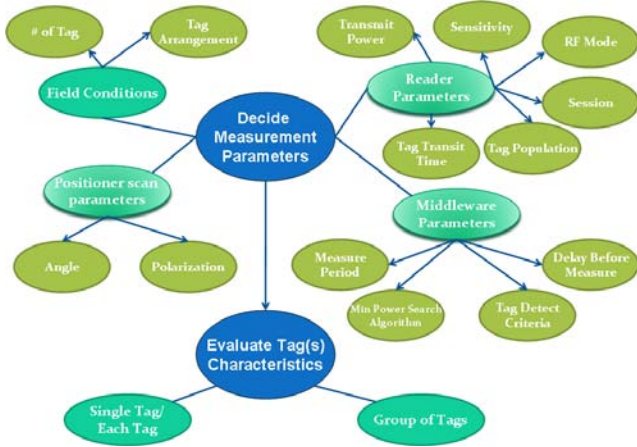


Fig. 5 Scope of measurement methodology.

III. MEASUREMENT METHODOLOGY

A. Measurement Period Optimization

Due to the relatively low RF performance characteristics restricted by the low product cost of the RFID tags, certain level of the error rate exists during the measurements [6]. An approach to minimize the error rate is to make the measurement period longer [7]. However, it will impact the measurement efficiency. An analysis on relationship between the measurement period and error rate to get a certain level of confidence on measurement results and measurement efficiency is discussed below.

Selection of the measurement period for each set of the measurement parameters depends on the total measurement period and the requirement on the measurement accuracy. A worst case measurement scenario of the multi-tag arrangement was performed to obtain the relationship between the measurement period and the error rate. In this scenario, five identical tags were parallel aligned closely as shown in Fig. 6(b) in such a way that there were strong mutual coupling among the tags which made individual tag hard to be identified compared to a stand-alone tag. The coarse mode with 30-degree angular spacing samples along theta and phi directions was made for the responses of the tags over the 3D sphere in both polarizations. In the experiment shown in Fig. 6, six fixed transmit power states, each differs by 3dB below the previous power state, were measured for each angle of observation. Although

the minimum power level step of Impinj reader is just 0.25dB, considering a measurement period of several seconds for detecting tag at every power level state, we have applied the much larger step to balance between measurement time and accuracy. Also, the tag detected criteria is defined as the number of tag reads greater than 12 and within a measurement period of 20 seconds. The initial probability distribution was made based on tag detected criteria defined above, as shown in Fig. 6. In a total of 864 (72*2*6) measurement trials, the effective measurement trials (the trials that detect any tag) are 168. Figure 6 (a) shows the possibility to detect more tag for the 168 effective measurement trails versus the measurement time period. Based on those experimental results, a convergence condition with the measurement period of 5 seconds results in a stable 98% confidence level of detecting tags. Also, the measurement period of 3 seconds yields an acceptable 95% confidence level of detecting tags.

TABLE II lists the total measurement time consumed for both the measurement periods of 3 and 5 seconds by using a Binary Search Algorithm to be described later. For the 95% measurement confidence level, the long measurement time shown in TABLE II indicates the requirement of having a practical approach to reduce the total measurement time for performing reliable measurements. As an example, in a similar measurement scenario applied in the OTA (over the air) performance evaluation of the mobile stations [8], a parameter referred as near horizon partial radiation sensitivity has been used to characterize the integrated receiver sensitivity of the mobile station over ± 30 or ± 45 degrees of the elevation angles from the horizon. Based on the reduced range of angular integration from ± 90 degrees to ± 30 or ± 45 degrees, it will effectively reduce the total measurement time approximately by a factor of 2/3 or 1/2, respectively yet still obtain the dominant performance/characteristics of the mobile station. Similar reduced scheme of measurement for the 3D tag readable range measurement may also be applied.

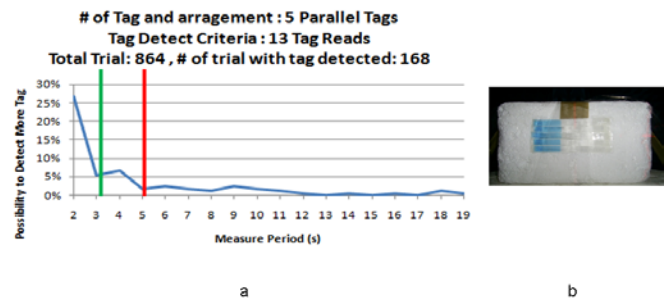


Fig. 6 Selection of measurement period (a) possibility to detect more tags vs. measurement period (b) tag arrangement in the RFID static system

TABLE II
ESTIMATION OF TOTAL MEASUREMENT TIME FOR BINARY SEARCH






	Estimate # of Measurement	Measurement Time In 3 seconds	Measurement Time In 5 seconds
Coarse	6 * 12 * 2 * 6 = 864	1hr 8 min	1hr 37min
Fine	12 * 24 * 2 * 6 = 3,456	3hr 17min	5hr 13min

B. Minimum Power Search Algorithm

In order to calculate the tag readable range, it is necessary to find an efficient algorithm for the minimum power search to get the minimum tag activation power. Three algorithms are implemented, as described below:

- 1) Each power search algorithm: detection of minimum tag activation power using each power level supported by the RFID reader. The reader output power is subsequently stepped down in a given step. Every tag in the group of the tags is monitored for being able to be detected at each reader output power level. During the course, the minimum tag activation power of every tag can be individually determined. However, it's the most time consuming algorithm.
- 2) Binary search algorithm: Instead of finding the minimum tag activation power to detect tag by each power level, a binary search approach is applied. For this method, the basic assumption is that the larger the reader transmit power, the greater the ability to detect tag. Thus, the number of measurement runs required for each angle and polarization to find the minimum tag activation power to detect the tag becomes $\log_2 n$, where n represents the number of the transmit power levels that the RFID reader supports.
- 3) Hierarchical search algorithm: This is a hybrid method of the above two algorithms. This approach assumes that if the transmit power difference is greater than 3dB, the higher the transmit power is, the greater the ability to detect tag will be. Thus, the binary search is applied with a 3dB step to find a rough solution first, and then each power search algorithm is employed within the 3dB range of the rough solution to obtain the accurate result. Here, the 3dB power search step is consistent with the six fixed transmit power states used for 15dB power range of adjustment available for Impinj reader based on the consideration described in the previous subsection.

Figure 7 demonstrates some results of those search algorithms. A conclusive remark can be made that for accuracy sensitive measurement requests, the hierarchical search algorithm shall be applied, while for time consumption sensitive measurement requests, the binary search algorithm shall be applied.

Min Power Search Algorithm	Confidence Level	Measure Time (Coarse Sampling)	Remark
Measure by Each Power	100% 	7 hr 45 min	
Binary Search	99.77% 	1 tag : 35 min 3 tags: 52 min 5 tags: 56 min	 Error happen inside 1.75 db
Hierarchical Search	100% 	1 tag : 2 hr 37 min 3 tags: 3 hr 40 min 5 tags: 3 hr 39 min	 Max error allowance within 3dB

Item	Total Iteration	Total Error	Error for Detect any	Error for Detect All
Test #	8748	20	13	3
Error rate %		0.23%	0.15%	0.03%

30 Degree Coarse Angle, 5 parallel tags, each power search for 3 times

Fig. 7 Comparisons of minimum power search algorithms

C. Characterizing maximum readable range

Though the NSI 3D scanner features a constant scan radius of 1.39 meter which prohibits the possibility of changing the distance between the probe antenna to the mast of supporting DUT with tags during measurements. The analogue of the equivalent range test distance versus measured power difference of the received power to the transmitted power from the reader antenna through Friis transmission formula in free space is applied in the anechoic chamber, as given by

$$R_{fix} = \frac{\lambda}{4\pi} \sqrt{\frac{EIRP_{fix} G_r}{P_{tag(threshold)}}} \quad (1)$$

where R_{fix} is the fix distance between the probe antenna and the tag, $EIRP_{fix}$ is the effective isotropic radiated power (EIRP) of the reader that downlinks to initially activate the tag, G_r is the antenna gain of the tag, and $P_{tag(threshold)}$ is the threshold power received by the tag to be just activated. The passive tag with the forward link being the bottleneck is considered here. Thus, the tag readable range is obtained by determining the minimum tag activation power through adjusting the transmit (downlink) power of the RFID reader [9]. The maximum readable range can then be evaluated by the following equation

$$R_{max} = R_{fix} \sqrt{\frac{EIRP_{max}}{EIRP_{fix}}} \quad (2)$$

where $EIRP_{max}$ is the maximum EIRP of the reader regulated by laws.

D. Polarization and Combination

The dual-polarized probe antenna in the 3D RFID test chamber supports two linearly polarized field component measurements in the directions of Theta and Phi, respectively [8]. During the process of the static test, the polarization is switched by a high-speed SPDT RF switch to measure the two mutually perpendicular polarization responses of the tag through which the associated response can be evaluated for a given reader antenna. Since the tag readable range is determined at the minimum EIRP level to activate tag, for a linearly polarized tag antenna as usually employed, the two measured minimum EIRP levels ($EIRP_\theta$ and $EIRP_\phi$) can be used to de-

termine the minimum EIRP level under a polarization match condition ($EIRP_t$) for evaluating the maximum readable range. Because $EIRP_\theta$ and $EIRP_\phi$ are proportional to the minimum tag activation power calibrated respectively with the polarization mismatch losses, as depicted in Fig. 8, $EIRP_t$ is simply given by the parallel combination of $EIRP_\theta$ and $EIRP_\phi$ shown below:

$$EIRP_t = \frac{EIRP_\theta \times EIRP_\phi}{EIRP_\theta + EIRP_\phi} \quad (3)$$

As for a circularly polarized reader antenna, the above $EIRP_t$ should be doubled.

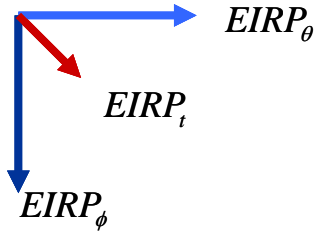


Fig. 8. Combination of the two measured minimum EIRP levels to determine the minimum EIRP level under the polarization match condition.

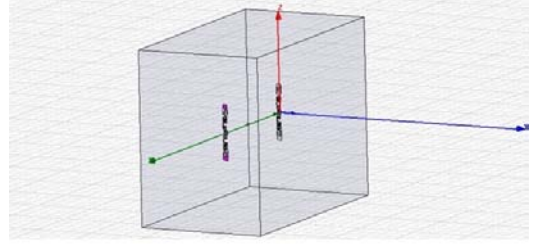
E. Inter-Tag interference measurement and simulation verification

Some results about inter-tag interferences are discussed in [10]. For measuring tag interference effects, the static test system had been applied by setting a tag population value to be the same as the number of tags measured and following the 3-second measurement period for the 95% confidence level. Thus, the collision or Q value effects of the RFID protocol layer should have been minimized. Therefore, the measurement results should be dominated by field interference effects among tags. As an example and also for verification, inter-tag interference measurements at tag-to-tag distances of 4, 12, 20, and 28 cm were performed with the static test system and compared with HFSS [11] simulations.

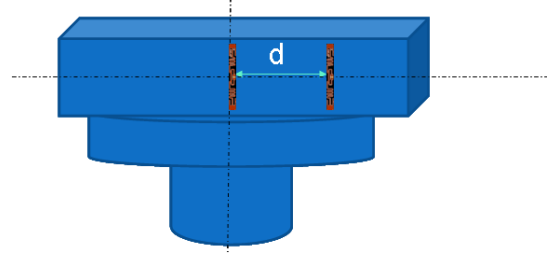
For those simulations, inter-tag interference for Alien 9540 tag mounted with Higgs-2 IC [12] was modeled by simulating interference introduced by two identical tags in free space. Voltage excitation was added to one of the tags whereas lump impedance was attached to the other tag to replace and model the tag IC's. The radiation patterns with the mutual coupling of two tags have been simulated with the HFSS. The impedance of the IC was modeled as an equivalent circuit formed by a parallel resistance of 1500Ω and a 1.2-pF capacitor at 922 MHz , i.e., $Z_{\text{chip}} = 13.7 - j143$. [13] Also, tag readable range measurements were performed along the horizontal plane ($\theta = 90$ degrees), as shown in Fig. 9. Fairly consistent results had been obtained between measurements and simulations.



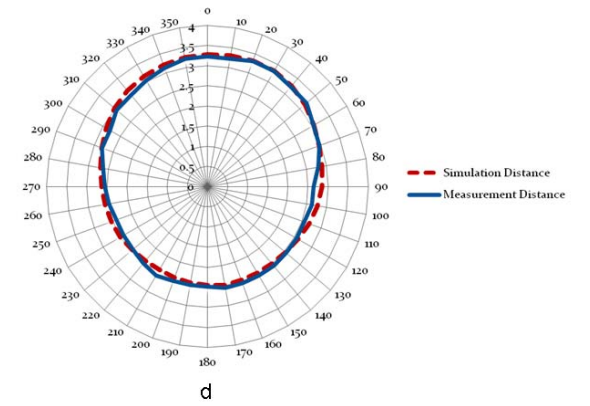
a



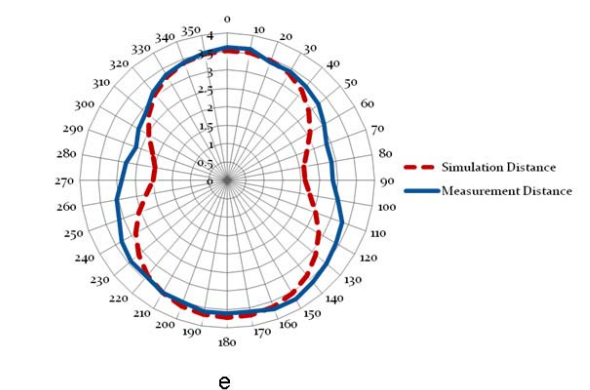
b



c



d



e

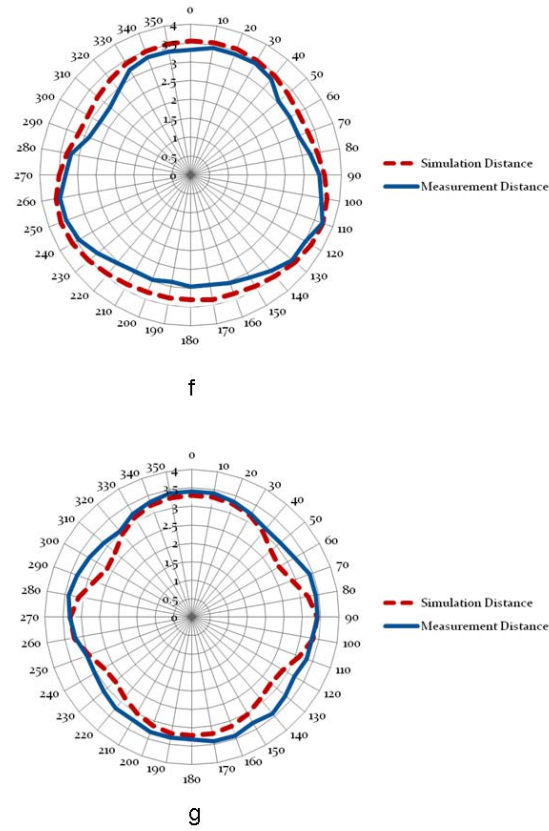


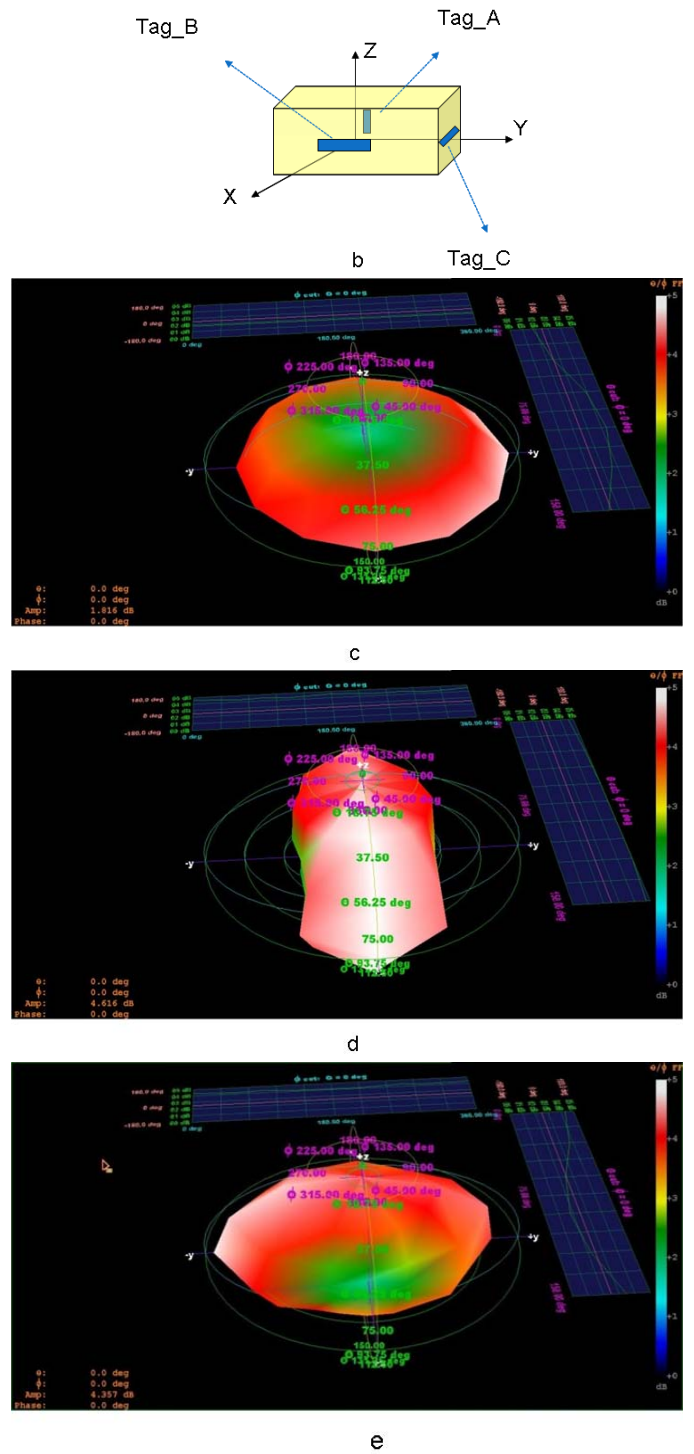
Fig. 9 Inter-tag interference measurements and simulations for the maximum readable range in $\theta=90^\circ$ plane. (a) measurement setup in the RFID static system (b) model in the HFSS (c) 3D model (d) measurement results for $d=40\text{mm}$ (e) measurement results for $d=120\text{mm}$ (f) measurement results for $d=200\text{mm}$ (g) measurement results for $d=280\text{mm}$

F. Validation of multiple tag measurements

Multiple tags can be measured simultaneously in a single scan with the static test system. As an example, three identical tags oriented in three mutually perpendicular directions were affixed on the sides of a rectangular Styrofoam block on the DUT support mast as shown in Fig. 10, together with measurement results for the “Detect All”, “Detect Any”, and “Detect Each” cases described previously. In the case of “Detect Each”, the 3D tag readable range results associated with those tags are consistent with the radiation pattern of the dipole-like tag antenna. The small 3D readable ranges for the “Detect All” case in Fig. 10 (f) and the isotropic readable range for the “Detect Any” case in Fig. 10 (g) are also reasonable for this example.



a



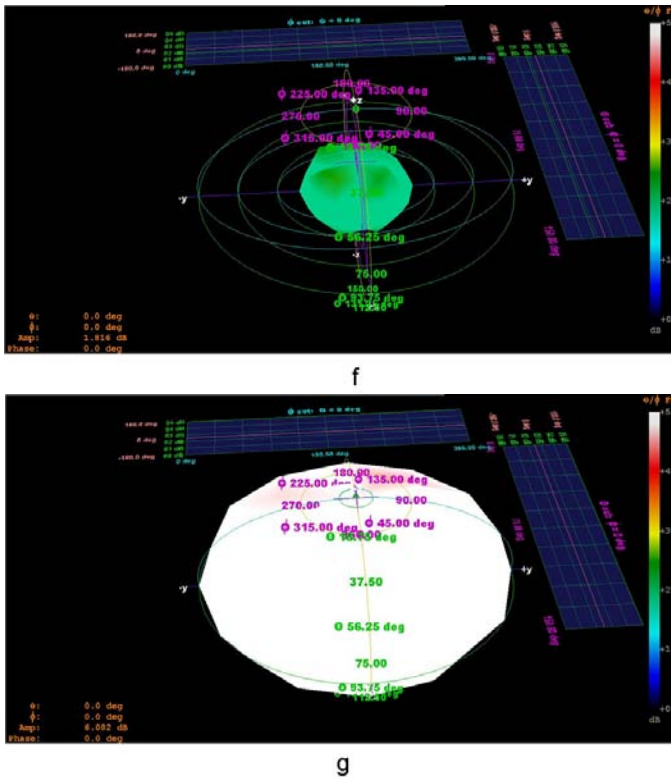


Fig. 10 An example of multiple tag measurements (a) tag measurement setup in the RFID static system (b) 3D model for tag deployment (c) 3D readable range of Tag_A (d) 3D readable range of Tag_B (e) 3D readable range of Tag_C (f) 3D readable range of the Detect All case (g) 3D readable range of the Detect Any case

IV. APPLICATIONS AND DISCUSSIONS

A. Transmit Power and read rate

While subsequently adjusting the transmit power of the RFID reader, an unusual symptom was observed, which had affected the read rate associated with the RFID tags in both cases of detecting a single isolated tag and detecting every individual tag response of five parallel grouped tags as shown in Fig. 11. Those measurement results indicate the impacts on read rate at different levels of transmit power for the two cases of detecting five parallel grouped tags and detecting a single isolated tag.

Based on the measured read rate results of the single isolated tag, it was found that as the transmit power was above certain threshold, the read rate retained at a certain range of level with minor variations. However, as the transmit power reduced below certain threshold, the associated read rate dropped suddenly.

Whereas the results of the read rate due to every individual tag response of five parallel grouped tags indicate that while one of five tags reaches the tag's readable power threshold, the read rates associated with the other four tags raise up as a result of the data bandwidth of communications occupied by the tag above the readable power threshold being released and applicable to the other tags. Also, the last readable tag survived till the lowest reader transmit power is the one located at the outermost and closest to the reader, as expected.

The mechanism remained in effect until the transmit power dropped under the readable power threshold of the last tag of the five parallel grouped tags as shown in Fig. 11. Notably, however, the read rate recorded for every tag of the five parallel grouped tags is less than the read rate recorded in the case of the single isolated tag. Possible explanation of this symptom might be attributed to the interference effects of the backscattered signals among multiple tags or the limitation of the available bandwidth for wireless communication between the reader and all associated tags.

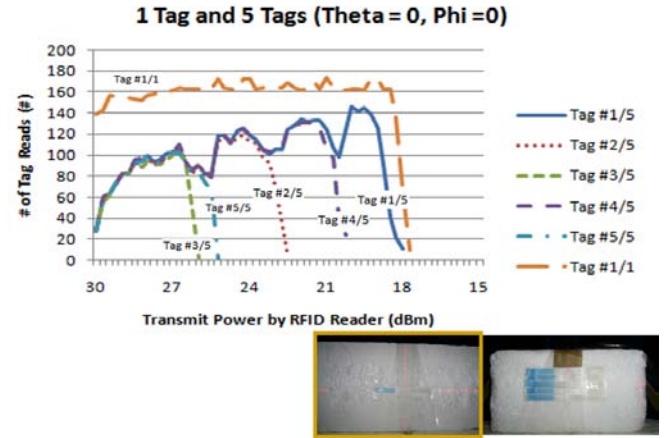


Fig. 11. Transmit power and number of tag read

B. Tag Readable Coverage

An effective indicator on the evaluation of the tag readable coverage can be evaluated from the ratio between the integrated tag detectable solid angle coverage and the whole detectable spherical solid angle coverage. The tag readable coverage rate had been evaluated over the entire detectable spherical solid angle based on the two tag grouping scenarios defined previously, "Detect Any" and "Detect All" modes by subsequently attaching stacked tags up to a total of 15 stacked tags as shown in Fig. 12. The two tag readable coverage curves shown in Fig. 12 indicate that there are two inflection points found in the cases of applying 5 stacked tags and 10 stacked tags associated with the "Detect All" grouping scenario and there is one inflection point found in the case of applying 10 stacked tags associated with the "Detect Any" grouping scenario. In those cases, the applied reader output EIRP had been kept at 1.6W, the maximum EIRP allowed in Taiwan. The effects of the interferences among tags are significant, particularly for the "Detect All" grouping scenario.

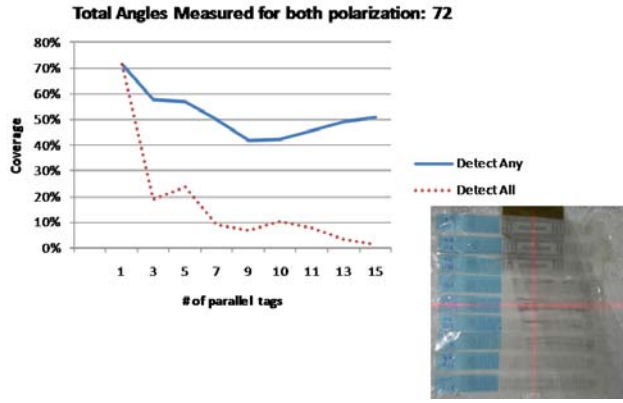


Fig. 12 Tag readable coverage rate versus number of stacked tags

C. 3D readable range measurements for tags on packages

One tag adhered on a package containing a circuit board was chosen to demonstrate the 3D readable range measurements using the static test system of Taiwan Tech. The measurement results are depicted in Fig. 13, which indicates the shielding and reflection effects of the PCB board on the tag.

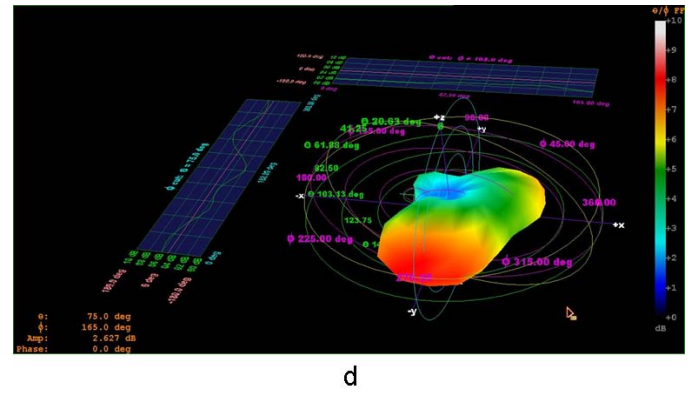
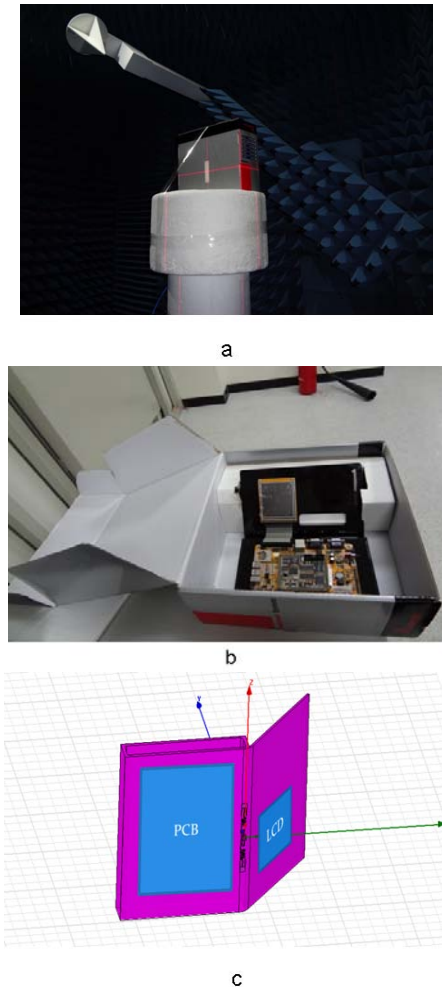
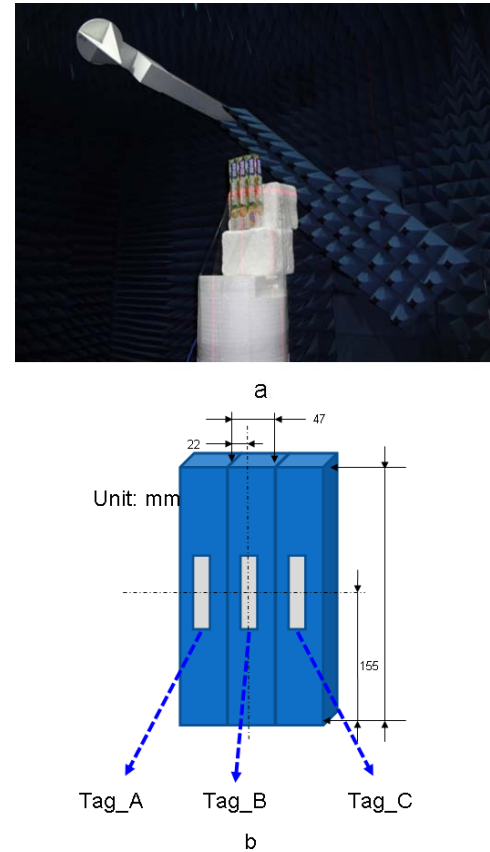


Fig. 13 Readable range measurements for a circuit board package (a) measurement setup in the RFID static system (b) circuit board package photo (c) 3D model for tag position in a circuit board package (d) 3D readable range pattern of the circuit board package

Another tag 3D readable range measurement instance was performed by adhering three identical tags each on the center of every one of the three packaged plastic wraps, as depicted in Fig. 14. The tag 3D readable range plots associated with the three tags are also shown. All three cases of the tag grouping scenarios, “Detect Any”, “Detect Each”, and “Detect All”, are demonstrated. Those results exhibit the effects of the boxes and adjacent tags on the 3D readable range, which can be obtained by applying the 3D RFID static test system.



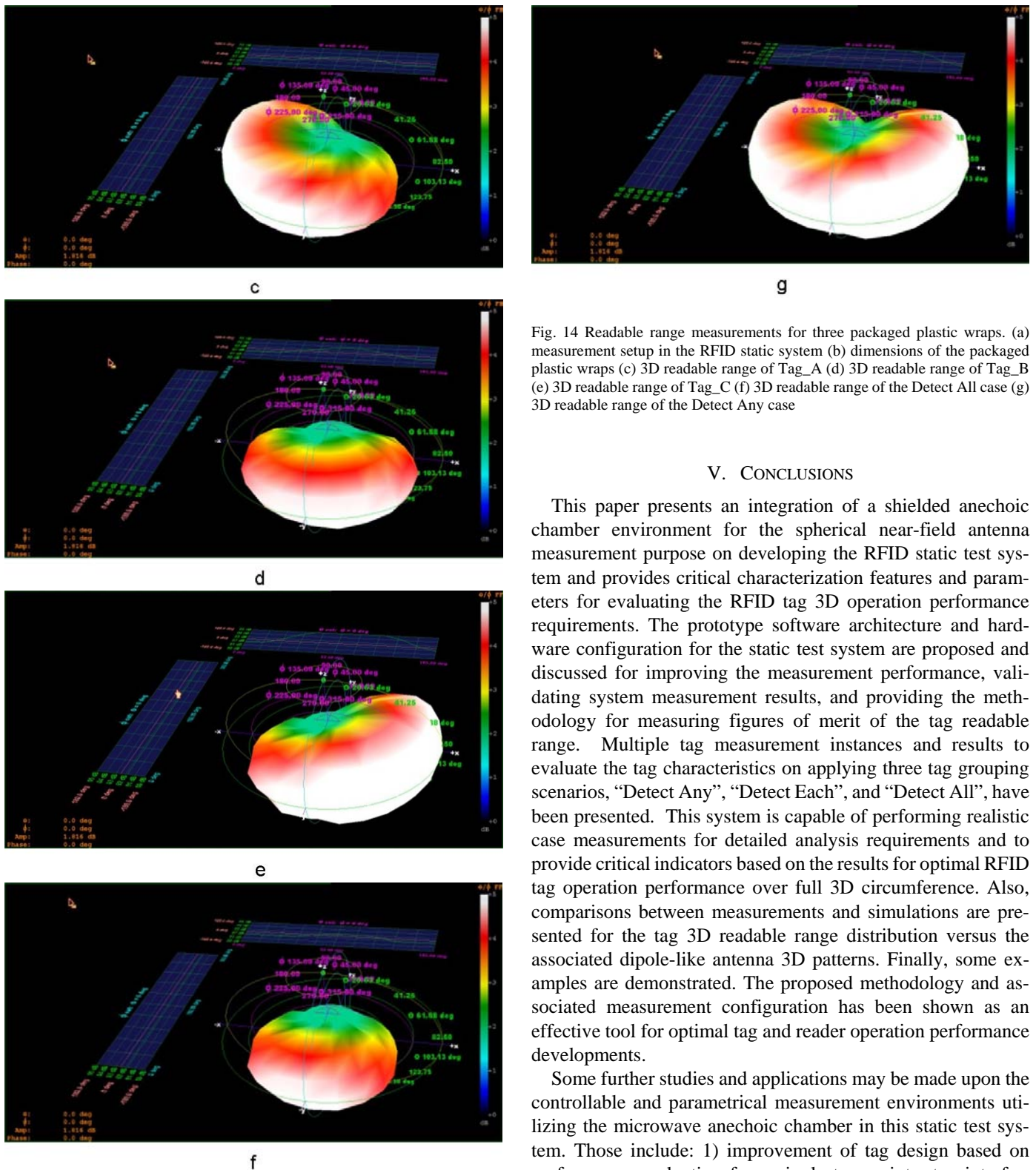


Fig. 14 Readable range measurements for three packaged plastic wraps. (a) measurement setup in the RFID static system (b) dimensions of the packaged plastic wraps (c) 3D readable range of Tag_A (d) 3D readable range of Tag_B (e) 3D readable range of Tag_C (f) 3D readable range of the Detect All case (g) 3D readable range of the Detect Any case

V. CONCLUSIONS

This paper presents an integration of a shielded anechoic chamber environment for the spherical near-field antenna measurement purpose on developing the RFID static test system and provides critical characterization features and parameters for evaluating the RFID tag 3D operation performance requirements. The prototype software architecture and hardware configuration for the static test system are proposed and discussed for improving the measurement performance, validating system measurement results, and providing the methodology for measuring figures of merit of the tag readable range. Multiple tag measurement instances and results to evaluate the tag characteristics on applying three tag grouping scenarios, “Detect Any”, “Detect Each”, and “Detect All”, have been presented. This system is capable of performing realistic case measurements for detailed analysis requirements and to provide critical indicators based on the results for optimal RFID tag operation performance over full 3D circumference. Also, comparisons between measurements and simulations are presented for the tag 3D readable range distribution versus the associated dipole-like antenna 3D patterns. Finally, some examples are demonstrated. The proposed methodology and associated measurement configuration has been shown as an effective tool for optimal tag and reader operation performance developments.

Some further studies and applications may be made upon the controllable and parametrical measurement environments utilizing the microwave anechoic chamber in this static test system. Those include: 1) improvement of tag design based on performance evaluation for a single tag or inter-tag interferences, 2) qualification of tag manufacturing process according to critical figures of merit introduced, 3) optimization on tag attachment positions or multi-tag positioning and grouping arrangements, 4) emulation of the realistic multi-path fading environments on the characterization for the 3D readable range of a single tag or group of tags.

Furthermore, other approaches may be considered without

the use of the chamber environment by applying the same methodology to the realistic operation environments of the RFID systems. The use of real scale 3D spherical scanner shall be able to identify and evaluate optimized packaging, shipping, and stacking layouts of goods with attached tags or groups of tags to inspect possible detection blind spots that tags fail to response to readers in the realistic environments.

ACKNOWLEDGMENTS

This work was sponsored by WavePro Inc., Taiwan and the National Science Council of ROC.

REFERENCES

- [1] J. Landt, "The History of RFID," *IEEE Potentials*, vol. 24, no. 4, Oct.-Nov. 2005, pp. 8-11
- [2] *Static Test Method For Applied Tag Performance Testing*, EPCglobal, May 2008.
- [3] *Low Level Reader Protocol (LLRP)*, EPCglobal, 2007.
- [4] *Octane™ RFID Software*, Impinj, 2009
- [5] *NSI 2000 Script Manual*, NSI, 2003
- [6] G. Fritz, V. Beroulle, M.D. Nguyen, O. Aktouf, I. Parissis, "Read-Error-Rate evaluation for RFID system on-line testing," *IEEE 16th International Mixed-Signals, Sensors and Systems Test Workshop (IMS3TW)*, pp. 1-6, June 2010
- [7] N. Ahmed, R. Kumar, R. S. French, and U. Ramachandaran, "RF2ID: A Reliable Middleware Framework for RFID Deployment," in *proc. IEEE International Parallel and Distributed Processing Symposium (IOPPS)*, 2007.
- [8] *Test Plan for Mobile Station Over the Air Performance*, CTIA, 2011
- [9] P.V. Nikitin, K.V.S. Rao, S.F. Lam, V. Pillai, R. Martinez, and H. Heinrich, "Power reflection coefficient analysis for complex impedances in RFID tag design," *IEEE Trans. on Microwave Theory and Techniques*, pp. 2721- 2725, Jan 2005.
- [10] G. Marrocco, "RFID Grids - Part I: Electromagnetic Theory," *IEEE Trans. on Antennas Propagation*, pp. 1019 – 1026, March 2011
- [11] *High Frequency Structure Simulator (HFSS) v9.1*, Ansoft Corporation
- [12] *ALN-9540 Squiggle® Inlay product overview*, Alien Technology, 2007
- [13] Medeiros, C. R., Costa, J. R, and Fernandes, C. A., "Passive UHF RFID Tag for Airport Suitcase Tracking and Identification", *IEEE Antennas and Wireless Propagation Letters*, Vol. 10 pp.123 - 126, Mar. 2011



Yuan-Hung Lee was born in Taipei, Taiwan in 1969. He received the B.S. degrees in mechanical engineering, in 1992 and 1994, and the M.S. degrees in electrical engineering, in 2005 and 2008, respectively all from National Taiwan University of Science and Technology (Taiwan Tech), Taipei. and is currently pursuing the Ph.D. degree in electrical engineering at Taiwan Tech. His research interests include Chamber integration, RFID, RF testing system development and wave propagation



Meng-Ying Tsai was born in Taipei, Taiwan, R.O.C., in 1976. She received the B.S. degrees from National Taiwan University in information management, in 1994 and 1998, and the M.S. degrees from National Taiwan University of Science and Technology, Taipei in electrical engineering, in 2007 and 2011. Her research interests include Chamber integration, RFID, RF testing system development.



Chang-Fa Yang (M'92) received the B.S. degree from National Taiwan University in 1983, and the M.S. and Ph.D. degrees from The Ohio State University, Columbus, USA in 1988 and 1992, respectively, all in electrical engineering. Then he joined the faculty in the Department of Electrical Engineering, National Taiwan University of Science and Technology (Taiwan Tech), and has been a professor since 1999. He has been the director of Wireless Communication and Electromagnetic Compatibility Research Center since 2005 and the chairman of the Electrical Engineering Department from 2009/8 to 2012/7 at Taiwan Tech. His research interests include antenna, wave propagation, RFID/IoT, high speed connector, and electromagnetic compatibility.



Ike Lin was born in Chiayi City, Taiwan in 1961. He received his B.S. and M.S. degrees of Physic in 1983 and 1985, respectively from National Central University, Taiwan. From 1985 to 2002, he served as a research specialist in various phase array antenna development and qualification programs by applying near-field antenna measurement metrology at Chung-Shan Institute of Science and Technology, Taiwan. Since January 1st, 2003 he has been with WavePro Inc focusing on implementing automated far-field/near-field antenna and RCS measurement facilities and has been actively supporting academic institutes and wireless industry manufacturers building up knowledge and proper measurement range solutions for the antenna performance characterization of wireless and microwave devices.